Available online at www.worldscientificnews.com

World Scientific News

WSN 32 (2016) 61-72 EISSN 2392-2192

3D-AFM Nano-structural Features and Magnetic Properties of Indium-Doped Vanadate Ceramic $Ca_{3-x}In_xVO_8$

Khaled M. Elsabawy

[a]Materials Science Unit Chemistry Department, Faculty of Science, Tanta University, Tanta - 31725, Egypt

[b]Materials Science Unit Chemistry Department, Faculty of Science, Materials Science Unit, Taif University, 888 - Alhawya, Taif City, Kingdom of Saudi Arabia

E-mail address: khaledelsabawy@yahoo.com ; ksabawy@yahoo.com

ABSTRACT

Doped vanadate ceramics with general formula $Ca_{3-x}In_xVO_8$ were synthesized by using two different precursors (oxalate & citrates) to get maximum homogeneity inside the bulk of the material where x = 0.05 and 0.25 mole. Structural and microstructural properties were monitoring by using both of XRD and SEM evaluating that indium doped - calcium vanadate ceramic has the semiconducting classical doubly perovskite phase as proved in the X-ray diffractogram, grain size of the material bulk was found to be in between 1.57- 2.23 μm which are lower than those reported in literatures .Magnetic measurements indicated that the In- doped- calcium vanadate ceramic exhibits an semiconducting behavior confirming that indium- hole dopings enhance the paramagnetic character and semi-conduction mechanism of the hexagonal perovskite phase. Furthermore 3D-AFM investigations were made to study effect of indium doping on the surface topology and grain size in the material bulk.

***Keywords*:** Solution route synthesis; X-ray diffraction; SE-microscopy; Semiconductors; Magnetic properties

1. INTRODUCTION

Oxides on the base of bismuth vanadate $Bi_4V_2O_{11}$*¡y* reveal the highest ionic conductivity among other oxides. So, they are intensively studied as promising for pure oxygen generation [1,2]. The parent bismuth vanadate compound undergoes phase transitions between ® and polymorphous modifications at approximately 700 K and between and tetragonal phase at approximately 850 K [3-5]. Composition modifications by substitution of different valency cations for V^{5+} and/or Bi^{3+} cations were aimed at and succeeded in the stabilization of the tetragonal structure phase at the room temperature [6-13].

However, the poor thermodynamic stability of these oxides in reducing atmospheres hinders their real applications and comprises the main task to be solved. The phase transitions and properties of ceramic solid solutions (Bi1*¡y*La*y*)4(V1*¡x*Zr*x*)2O11*¡z* with *x; y* < 0:2, have been studied [7-9]. By introduction of La^{3+} and Zr^{4+} cations , we intended to improve the thermodynamic stability of bismuth vanadate-based compositions [9].

Based on the electrical, magnetic and other related properties, there has been rapid progress in developing new materials of different structural families (i.e., perovskite, tungsten bronze, layer structure, etc.) for different devices, such as capacitors, actuators, pyro-electric detectors, transducers, electro-optic, ferroelectric random access memory and display, etc. [1-7]. Out of the materials developed only a few can be used in wireless communication technologies such as cellular phones, microwave multilayer integrated circuits, etc. [8-10]. In this attempt physical properties of some materials have been tailored either by substituting suitable elements at different atomic sites of the structure of the material or fabricating complex/composite systems [11-13]. Though a lot of complex systems now-a-days are available for the purpose, $CaO–Nb_2O_5$, $BaO–Nb_2O_5$, $SrO–Nb_2O_5$ binary systems [14] have been found very interesting and useful because of diversity of their crystal structural, stability and physical properties.

Some mixed metal oxides containing vanadium (V^{4+}) with perovskite-related structure have recently been found interesting as transition metal analogs of the cuperate superconductors and ionic conductors [15-25]. Although Nb^{5+}, Ta^{5+} and V^{5+} containing systems have recently been studied in details for different applications, not much has been reported on structural and electrical properties of $Ca-O–V_2O_5$ which is the subject of this paper.

The major goal in the present article is to investigate the effect indium-dopings on;

a) Structural and Nano-structural properties of In-doped $Ca_{3-x}In_xVO_8$ ceramics.

b) Electrical conduction and Magnetic properties of In-doped- $Ca_{3-x}In_xVO_8$ samples.

2. EXPERIMENTS

A. Samples preparation

The In-doped – vanadates ceramics with general formula $Ca_{3-x}In_xVO_8$ were selected from another study for authors to be the target of this investigation where x = 0.05 and 0.25 mole. The preparation was attempted by applying solution route and sintering procedure using the molar ratios of In_2O_3 ,V_2O_3, and $CaCO_3$ each of highly pure chemical grade purity. The mixture were ground carefully then solublize in few drops of concentrated nitric acid

forming nitrate extract which diluted by distill water. The nitrate solution was neutralized by using 30 % urea solution and pH becomes ~ 6. Mixture I was for calcium solution and mixture II was for (indium + vanadium) nitrates. Mixture I was diluted by distill water to be 100 ml then pH was adjusted to be 8.5 concentrated solution of oxalic acid was added carefully till heavy white precipitate from calcium oxalates is obtained and the pH must be higher than 8. The oxalate precursor is filtered and washed by 5 % ammonium nitrate solution. Mixture II of indium and vanadium was passing through the same treatment but citric acid was applied instead of oxalic in present of ethylene glycol as complexing agent to produce gelatinous precipitate of indium-vanadium citrates that formaing citrates precursor.

The calcium oxalate and In/V-citrates precursors were forwarded to muffle furnace and calcinations process was performed at 780 °C under a compressed O_2 atmosphere for 10 hrs then reground and pressed into pellets (thickness 0.2 cm and diameter 1.2 cm) under 6 Ton /cm^2. Sintering was carried out under oxygen stream at 900 °C for 20 hrs. The samples were slowly cooled down (20 °C /hr) till 500 °C and annealed there for 8 hrs. under oxygen stream. The furnace is shut off and cooled slowly down to room temperature. Finally the materials are kept in vacuum desiccator over silica gel dryer.

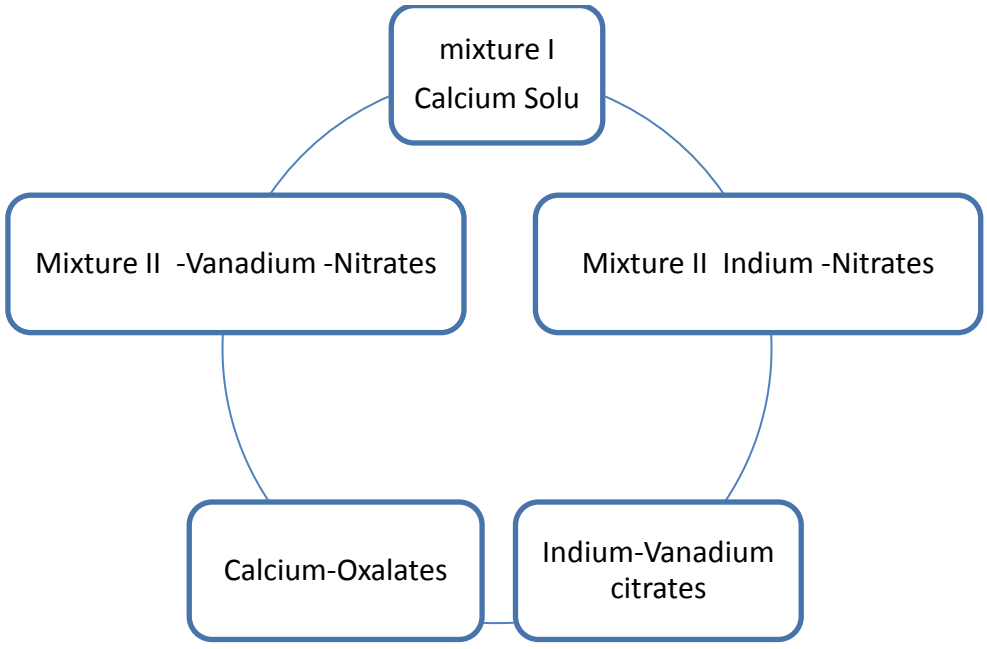

Schematic diagram show two different precursor applied for synthesizing Indium-doped vanadates.

B. Phase Identification

The X-ray diffraction (XRD) measurements were carried out at room temperature on the fine ground samples using Cu-K_α radiation source, Ni-filter and a computerized STOE diffractometer / Germany with two theta step scan technique. Scanning Electron Microscopy (SEM) measurements were carried out at different sectors in the prepared samples by using a computerized SEM camera with elemental analyzer unit (PHILIPS-XL 30 ESEM /USA).

Atomic force microscopy (AFM): High-resolution Atomic Force microscopy (AFM) is used for testing morphological features and topological map (Veeco-di Innova Model-2009-AFM-USA).The applied mode was tapping non-contacting mode. For accurate mapping of the surface topology AFM-raw data were forwarded to the Origin-Lab version 6-USA program to visualize more accurate three dimension surface of the sample under investigation. This process is new trend to get high resolution 3D-mapped surface for very small area ~ 0.1 x 0.1 μm^2.

C. Magnetic measurements

The cryogenic AC-susceptibility of the prepared materials was undertaken as a function of temperature recorded in the cryogenic temperature zone down to 30 K using liquid helium refrigerator.

3. RESULTS AND DISCUSSION

3. 1. Phase Identification

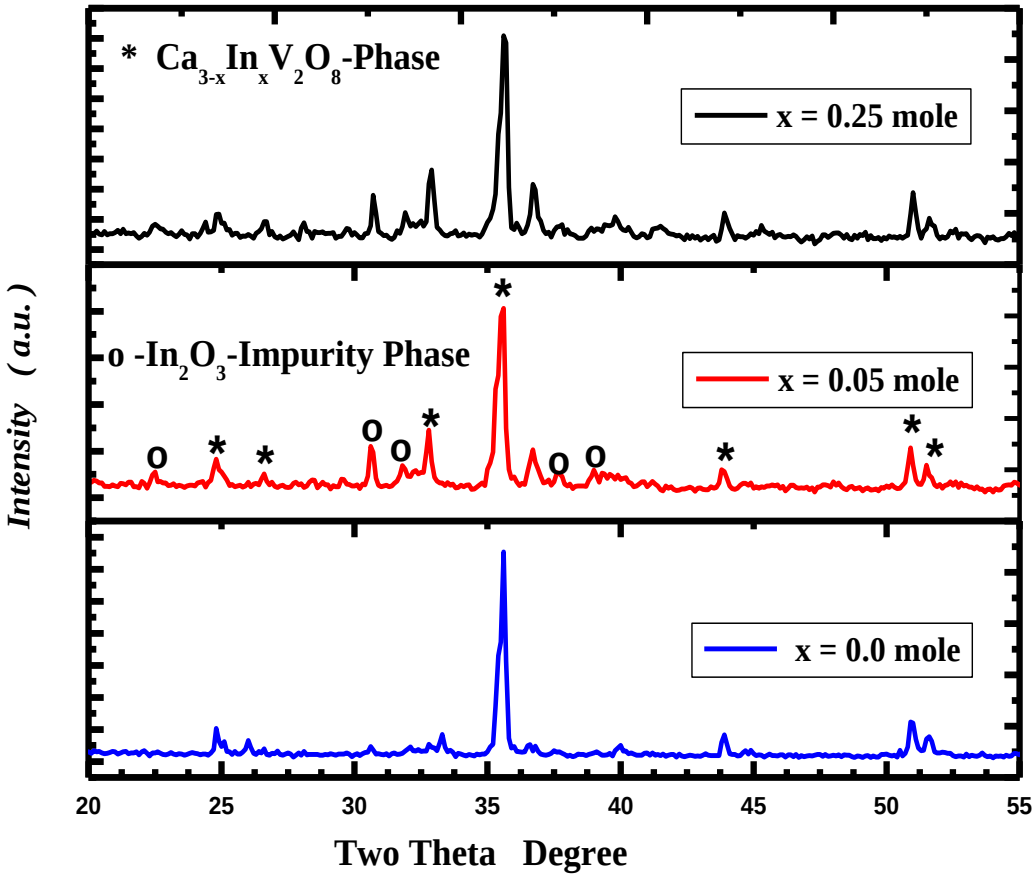

Fig. 1. X-ray diffraction pattern recorded for In-doped – vanadates ceramics with general formula $Ca_{3-x}In_xVO_8$; where x = 0.0, 0.05 and 0.25 mole.

Fig. 1(a-c): displays the X-ray powder diffractometry pattern for In-doped – vanadates ceramics with general formula $Ca_{3-x}In_xVO_8$ where x = 0.0 , 0.05 and 0.25 mole respectively. Analysis of the corresponding 2θ values and the interplanar spacings d (Å) were carried out and indicated that ,the X-ray crystalline structure mainly belongs to a single hexagonal doubly pervoskite phase $Ca_{3-x}In_xVO_8$ in major besides few peaks of In_2O_3 as secondary phase in minor. The lattice parameters of the unit cell were refined using the least-squares sub-routine of a standard computer program these refined lattice parameters are: $a = b = 16.8312$ Å, $c = 40.3783$ Å with estimated standard deviation in parenthesis. These unit cell parameters are in good agreement with those of the reported ones for $Ca_3Nb_2O_8$ structure [26].

The unit cell dimensions were calculated using the most intense X-ray reflection peaks which is fully agreement with those mentioned in the literature [27-29] .

It is obviously that, the additions of In_2O_3 has a negligible effect on the main crystalline structure hexagonal doubly pervoskite phase $Ca_{3-x}In_xVO_8$ with In-content (x = 0.25) as shown in Fig. 1(c). From Figs. 1(a,b) one can indicate that hexagonal pervoskite phase $Ca_{3-x}In_xVO_8$ is the dominating phase by ratio exceeds than 90 % confirming that In-ion substitutes successfully on the Ca-sit at low concentration x = 0 ,0.05 mole without damaging the original – pervoskite hexagonal phase.

Table.1,2 explain EDX-elemental analysis data recorded for $Ca_{3-x}In_xVO_8$ where x = 0.05 and 0.25 mole that prepared via solution route. It is clear that the atomic percentage recorded is approximately typical with the molar ratios of the prepared sample emphasizing the quality of preparation through solution technique.

On the basis of ionic radius In-ion can substitute on the ca-sites causing slight shrinkage in the lattice without destroying it as clearly appears in the x-ray diffractogram Fig. 1. since $Ca_{3-x}In_xVO_8$ hexagonal phase is clearly assigned in our x-ray patterns by * as shown in Fig. 1.

3. 2. SE-microscopy measurements

Fig. 2(a-c) show the SEM-micrographs recorded for In-doped – vanadates ceramics with general formula $Ca_{3-x}In_xVO_8$ where x = 0.0, 0.05 and 0.25 mole. The estimated average of grain size was calculated and found in between 1.57- 2.23 μm supporting the data reported in [23].

The EDX examinations for random spots in the same sample confirmed and are consistent with our XRD analysis for polycrystalline In-doped – vanadates ceramic sample, such that the differences in the molar ratios EDX estimated for the same sample is emphasized and an evidence for the existence of hexagonal phase with good approximate to molar ratios see (Table 1-3).

From Fig. 2(a-c), it is so difficult to observe inhomogeneitiy within the micrograph due to that the powders used are very fine and the particle size estimated is too small.

This indicates that, the actual grain size in the material bulk is smaller than that detected on the surface morphology. Furthermore, in our EDX (energy disperse X-ray) analysis, In^{3+} was detected qualitatively with good approximate to the actual molar ratio but not observed at vanadates ceramics grain boundaries which confirm that, indium(III) has diffused regularly into material bulk of superconducting vanadates ceramics - phase and In-ion induces in the crystalline structure through solid state reaction by some extent. The inclusion of In-ion is confirmed also by the enhancing the semiconducting behavior of vanadates ceramics semiconductor.

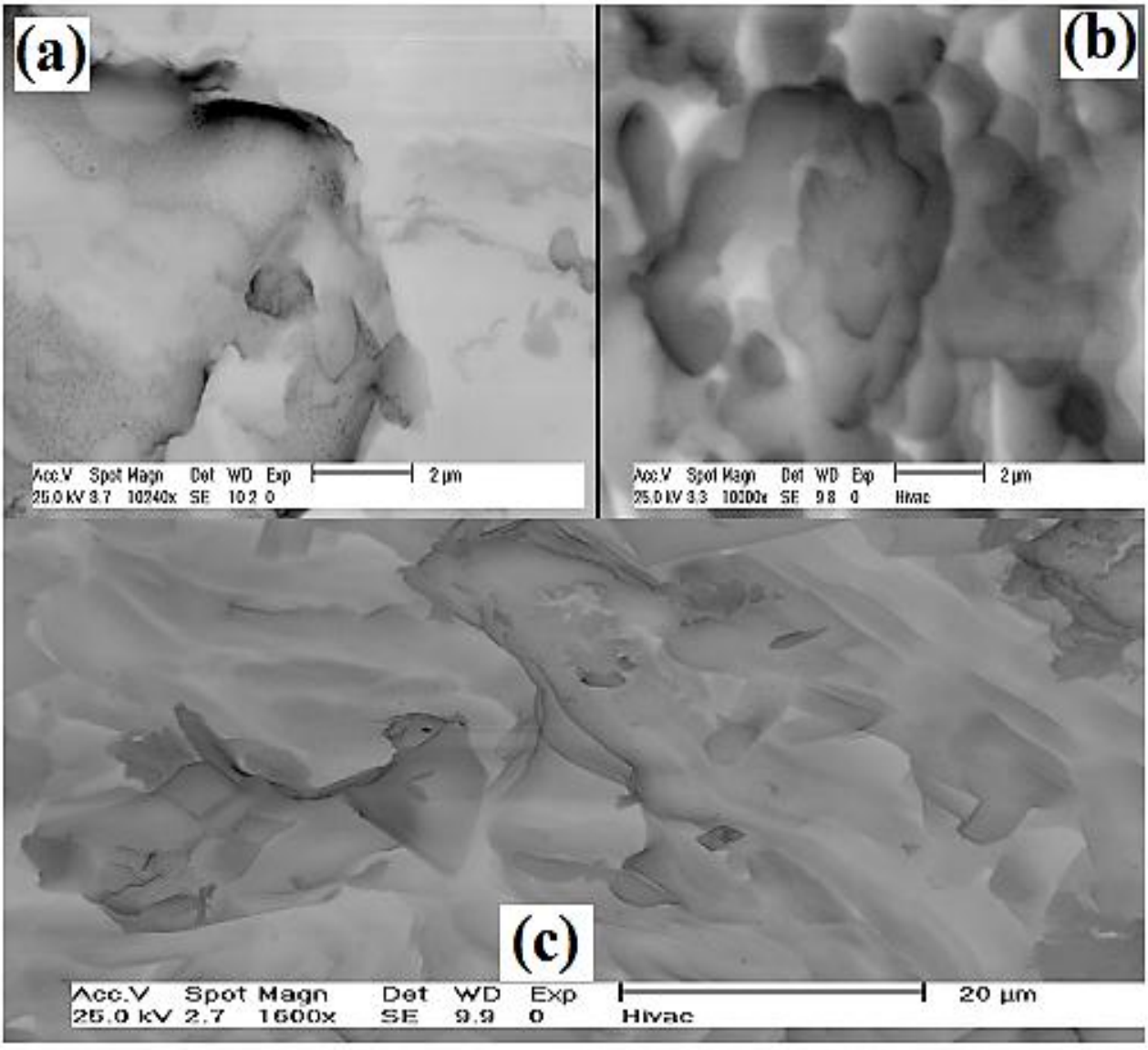

Fig. 2(a-c). SE-Micrographs recorded for In-doped – vanadates ceramics with general formula $Ca_{3-x}In_xVO_8$; where; (a) x = 0.0, (b) x = 0.05 and (c) x = 0.25 mole, with different magnification factors 2 and 20 µm.

Table 1. EDX-elemental analysis recorded for Ca_3VO_8 system.

	Ca_3VO_8					
Element	**Wt %**	**At %**	**K-Ratio**	**Z**	**A**	**F**
O K	**65.39**	**60.15**	**0.1137**	**1.1219**	**0.7131**	**1.0019**
V K	**7.23**	**9.139**	**0.0139**	**1.2443**	**0.2253**	**1.0011**
CaK	**24.26**	**30.53**	**0.1931**	**1.0336**	**0.5507**	**1.0313**

Table 2. EDX-elemental analysis recorded for $Ca_{2.95}In_{0.05}VO_8$ system.

	$Ca_{2.95}In_{0.05}VO_8$					
Element	**Wt %**	**At %**	**K-Ratio**	**Z**	**A**	**F**
O K	**65.38**	**60.15**	**0.1037**	**1.1119**	**0.7131**	**1.0019**
V K	**7.29**	**9.139**	**0.0159**	**1.2443**	**0.2253**	**1.0011**
CaK	**23.26**	**30.48**	**0.1831**	**1.0336**	**0.5507**	**1.0313**
In L	**0.1606**	**0.145**	**0.0332**	**0.9481**	**1.0218**	**1.0118**

Table 3. EDX-elemental analysis recorded for $Ca_{2.75}In_{0.25}VO_8$ system.

	$Ca_{2.75}In_{0.25}VO_8$					
Element	**Wt %**	**At %**	**K-Ratio**	**Z**	**A**	**F**
O K	**63.32**	**61.15**	**0.1247**	**1.1259**	**0.8131**	**1.0022**
V K	**8.21**	**9.189**	**0.0149**	**1.1563**	**0.2252**	**1.0021**
CaK	**21.26**	**29.87**	**0.1731**	**1.0126**	**0.5607**	**1.0213**
In L	**0.706**	**0.645**	**0.0352**	**0.8721**	**1.0518**	**1.0123**

3. 3. Magnetic and electrical properties

Fig. 3(a-c) exhibits magnetic susceptibility curve recorded as a function of absolute temperatures for vanadates ceramics samples synthesized via solution route. It is clear that the conduction increases as temperatures raise reflecting semiconductor behavior for vanadates ceramic sample. Although the indium dopant has metallic behavior as reported in literatures [22-25] it enhances semi-conduction mechanism inside material bulk of vanadates ceramics. From this point of view indium as dopant element with metallic character expected to make a shift towards semiconducting behavior as achieved in our investigation.

Transport properties of the materials obeying Arrhenius equation $\sigma_{ac} = \sigma_0 \exp(-E_a/K_B T)$, where the symbols have their usual meanings. It is observed that the ac conductivity of the material increases with rise in temperature, and shows the negative temperature coefficient of resistance behavior. The values of activation energy of the compound are found to be 0.18, 0.20 and 0.23 eV for x = 0.0 ,0.05 and 0.25 mole respectively.

This behavior suggests that the conduction mechanism of the compound may be due to the hopping of charge carrier that enhanced by indium holes- dopings and the energy gabs between conduction and valence band increase as In-dopant concentration increase as shown in Fig. 4.

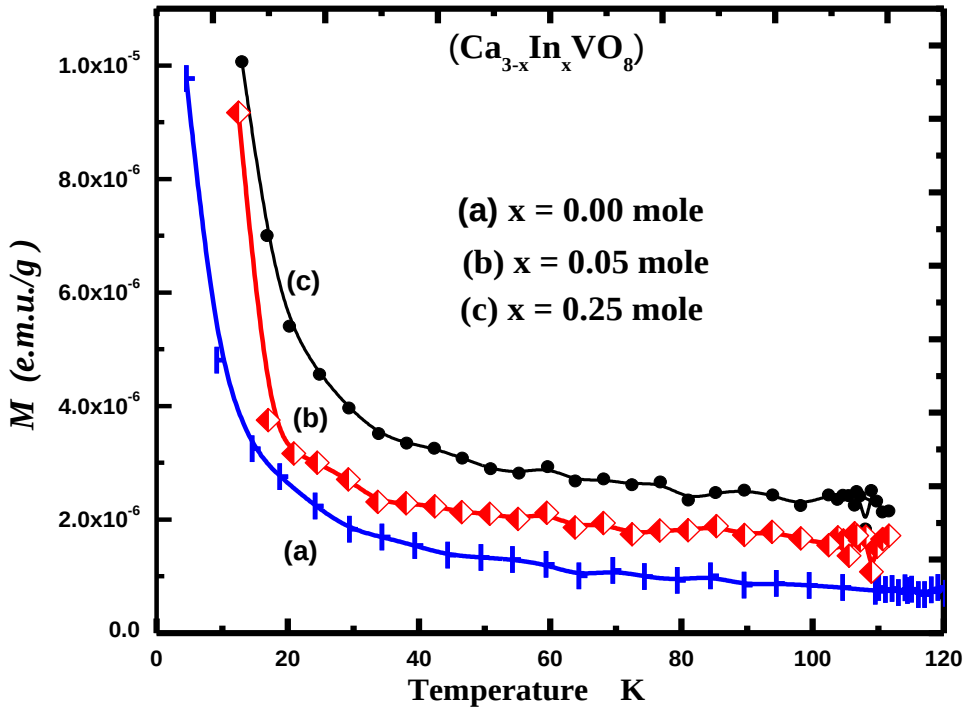

Fig. 3(a-c). Magnetic susceptibility curve recorded for In-doped – vanadates ceramics with general formula $Ca_{3-x}In_xVO_8$; where: (a) x = 0.0 , (b) x = 0.05 and (c) x = 0.25 mole.

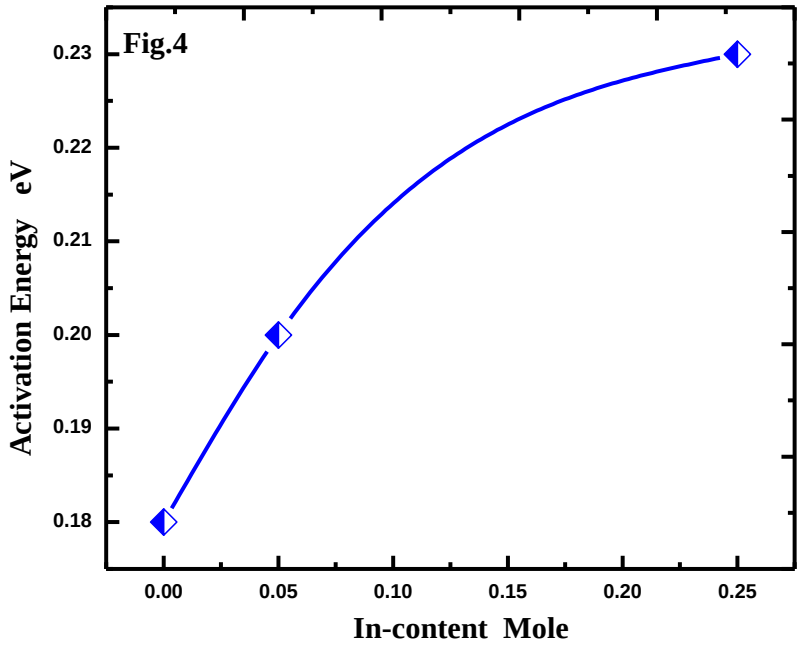

Fig. 4. Activation energies calculated for indium doped ceramics versus In-content.

3. 4. Nano-Structural Properties

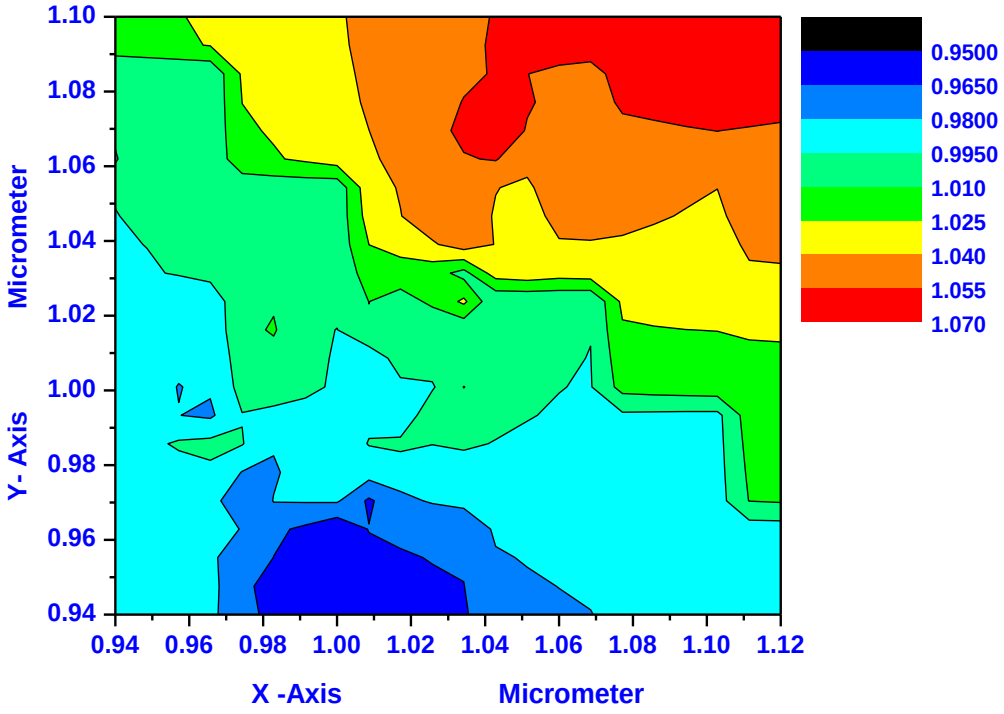

Fig. 5(a). 2D-visualized AFM-image for $Ca_{2.95}In_{0.05}VO_8$.

Fig. 5(a) shows 2D-AFM-visualized image for indium doped-vanadates ceramic applying non-contact tapping mode for very tiny area 0.18x0.18 μm^2. The analysis of surface topology indicated that ~ 40% of the surface heights lies in between 0.99-0.95 μm blue color zones while the maximum heights which represents nearly ~ 22% of the whole scanned area yellow-red colors zones. The differentiation on the surface topology reflect remarkable increase in the surface area in which most of technological applications are dependent on it as known and mentioned in literature [13-21].

For accurate analysis figure 5b was constructed by forwarding the raw data of AFM into origin lab program converting the data firstly into matrix then constructing three dimensional xyz as clear in Fig. 5(b) which describes 3D-AFM-visualized image for indium doped-vanadates ceramic applying non-contact tapping mode for very tiny selected area 0.18x0.18 μm^2.

The analysis of surface topology indicated that ~ 40% of the surface heights lies in between 0.99-0.95 μm blue color zones while the maximum heights which represents nearly ~ 22% of the whole scanned area yellow-red colors zones. The color gradient refers to differences in the heights levels which function on the average surface area [14-16].

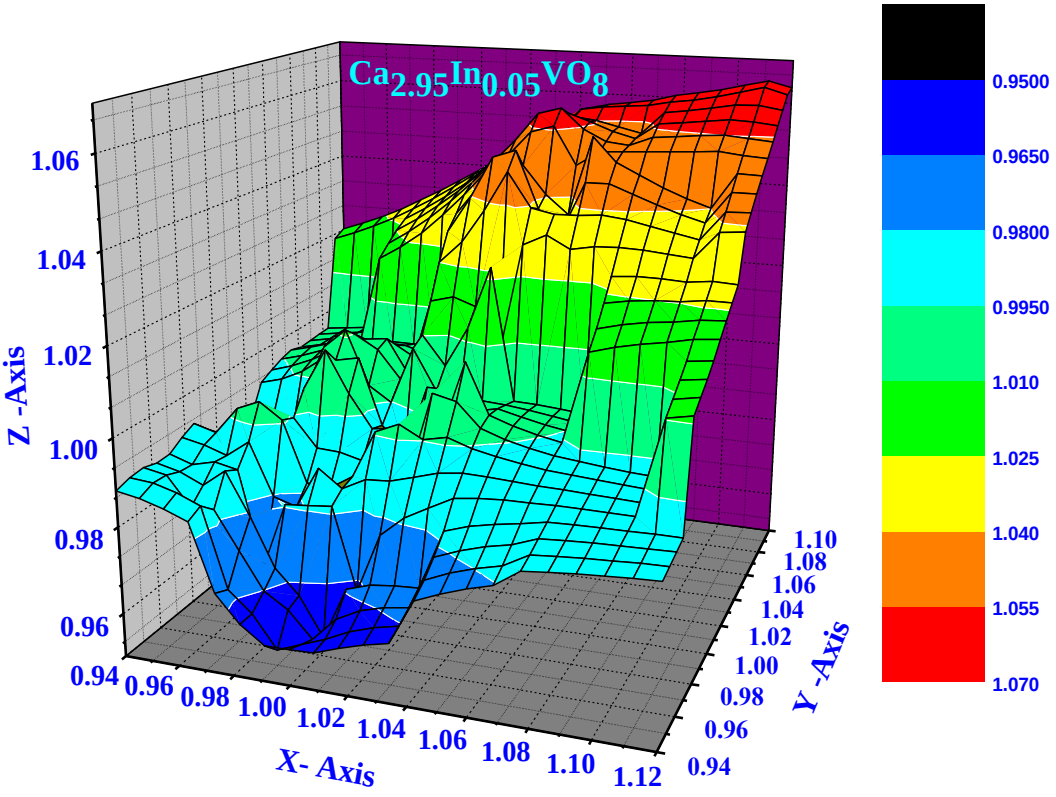

Fig. 5(b). 3D-AFM-image for $Ca_{2.95}In_{0.05}VO_8$.

4. CONCLUSIONS

The conclusive remarks inside this article can be summarized as the follow;

1- Solution technique exhibits structure quality as preparation technique.

2- In-dopant make a shift towards hexagonal phase

3- SE-micrographs confirmed that In-ions distribute regularly through out the lattice structure of vanadates ceramics without destroying hexagonal-phase.

4- Magnetic order of $Ca_{3-x}In_xVO_8$ (where x = 0.05 and 0.25 mole) does not changed and still semiconducting order although indium-dopant has metallic character.

5- The values of activation energy of the In-doped-ceramics are raised as indium increases.

6- AFM-investigations confirmed the data obtained from SE-microscopy.

References

[1] D. Szwagierczak and J. Kulawik, *J. Eur. Ceram. Soc.* 24 (2004) 1979.

[2] H. El Alaoui–Belghiti, R. Von der Mühll, A. Simon, M. Elaatmani and J. Ravez, *Mater. Lett.* 55 (2002) 138.

[3] N. Wakiya, J.K. Wang, A. Saiki, K. Shinaki and N. Mizutani, *J. Eur. Ceram. Soc.* 19 (1999) 1071.

[4] M.R. Raju and R.N.P. Choudhary, *J. Phys. Chem. Solids* 64 (2003) 847.

[5] X.M. Chen, Z.Y. Xu and J. Li, *J. Mater. Res.* 15 (2000) 125.

[6] L.G. Van Uitert, S. Singh and H.J. Levinstein, *Appl. Phys. Lett.* 11 (1967) 61.

[7] J.J. Rubin, L.F. Van Uitert and H.J. Levinstein, *J. Cryst. Growth* 1 (1967) 315.

[8] W. Wersing, Electronic Ceramics. In: B.C.H. Steele, Editor, Elsevier, New York (1991) Chapter 4.

[9] W. Wersing, *Curr. Opin. Solid State Mater. Sci.* 1 (1996) 715.

[10] T. Negas, G. Yeager, S. Bell and R. Amren, NIST special publication 804. In: P.K. Davies and R.S. Roth, Editors, NIST (1991), pp. 21-38.

[11] R.J. Cava, J.J. Krajewski and R.S. Roth, *Mater. Res. Bull.* 33 (1998) 527

[12] R. Umemura, H. Ogawa, A. Yokoi, H. Ohsato and A. Kan, *J. Alloy. Compd.* 424 (2006) 388.

[13] H. Ogawa, A. Yokoi, R. Umemura and A. Kan, *J. Eur. Ceram. Soc.* 27 (2007) 3099.

[14] L.M.D. Cranswick, W.G. Mumme, I.E. Grey, R.S. Roth and P. Bordet, *J. Solid State Chem.* 172 (2003) 178.

[15] H.-Zh. Li, L.-M. Liu, K.P. Reis and A.J. Jacobson, *J. Alloy. Compd.* 203 (1994), p. 181

[16] G. Xiao, F.H. Streitz, A. Gavrin, Y.W. Du , C.L. Chien, *Phys. Rev. B* 35, 8782 (1987).

[17] Y. Maeno, T. Tomita, M. Kyogoku, S. Awaji, Y. Aoki, K. Hoshino, A. Minami, T. Fujita, *Nature* 328, 512 (1987).

[18] J.M. Tarascon, P. Barboux, P.F. Maceli, L.H. Greene, G.W. Hull, *Phys. Rev. B*37, 7458 (1988).

[19] H. Renevier, J.L. Hodeau, M. Marezio, A. Santoro, *Pysica C* 220, 143 (1994).

[20] R.G. Kulkarni, D.G. Kuberkar, G. J. Baldaha, G.K. Bichile, *Physica C* 217, 175(1993).

[21] J.F. Bringley, T.M. Chen, B.A. Averill, K.M. Wong, S.J. Poon, *Phys. Rev. B*38, 2432 (1988).

[22] Y. Shimakawa, Y. Kubo, K. Utsumi, Y. Takeda, M. Takano, *Jpn. J. Appl. Phys.* 27, L1071 (2006).

[23] Z.Hiroi, M. Takano, Y. Takeda, R. Kanno, Y. Bando, *Jpn. J. Appl. Phys.* 27, L580 (1988).

[24] M.P. Delamare, M. Hervieu,I. Monot, K. Verbist and G. Tendeloo, *Physica C* 262, 220 (1996).

[25] P.N. Peters, R.C. Sisk. E. Ubran, C.Y. Huang and M.K. Wu *Appl. Phys. Lett*. 52, 2066 (1988).

[26] C.Y. Huang, Y. Shapiro, E.J. McNiff, P. N. Peters, B.B. Shwatrz, M.K. Wu, R.D. Shull and C.K. Chiang, *Mod. Phys. Lett.* 2, 869 (1988).

[27] J.P. Singh, H.L. Leu, R.B. Poepple, E. Voorhees, G.T. Goudery, K. Winsley and D. Shi *J. Appl. Phys.* 66, 3154 (1989).

[28] B. Dwir, M. Affronte and D. Pavuna, *Appl. Phys. Lett*. 55, 399 (1989).

[29] J. Jung, M.A. Mohammed, S.C. Cheng and J.P. Frank, *Phys. Rev. B*42, 6181 (1990).

(Received 26 November 2015; accepted 09 December 2015)